



# MABEL Flights out of NASA Langley supporting ICESat-2 Algorithm Development

William B. Cook, Code 612, NASA GSFC

The Multiple Altimeter Beam Experimental Lidar (MABEL) instrument recently completed an extremely successful flight campaign over vegetation, water and calibration targets in MD, VA, and NC. MABEL flew aboard the Scaled Composites Proteus aircraft using 4 science flights to collect over 20 hours of high-quality science data during September 2013. MABEL used a multi-beam photon counting technique to measure elevation and surface brightness over vegetation canopies, the Chesapeake Bay, Ocean City, SERC, and WFF runways (calibration).

- MABEL data are used to develop new science algorithms and data reduction methods for the ICESat-2/ATLAS instrument because ATLAS employs a photon counting lidar technique that differs from the waveform lidar technique used by ICESat/GLAS.
- The primary purpose of this campaign was to acquire vegetation canopy data and calibration data similar to that expected from ATLAS.
- Additionally, several engineering tests were performed, and data to enhance evaluation of the eventual ATLAS calibration techniques were acquired.

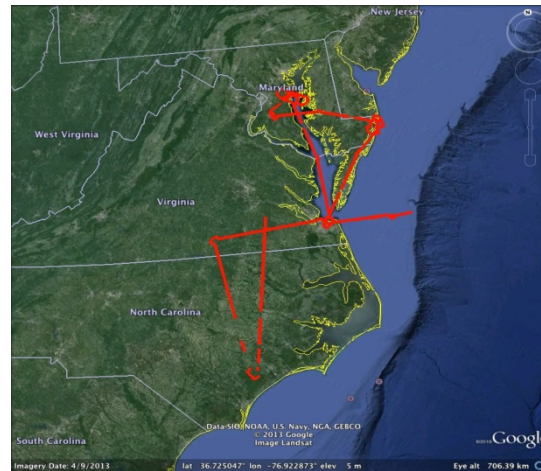


**Figure 1: Targets covered by MABEL during the recent deployment.** The same flight path was covered, under varying cloud conditions, for each flight. The red line above shows where surface was detected (i.e., little cloud interference) during one MABEL flight.



**Figure 3: Proteus returning to the LaRC hangar from a night flight.** This was MABEL's first campaign aboard Proteus. Two 5.5 hour flights were undertaken at night, and two 5.5 hour flights in the daytime. Lights in the background are on the USAF base and runway.

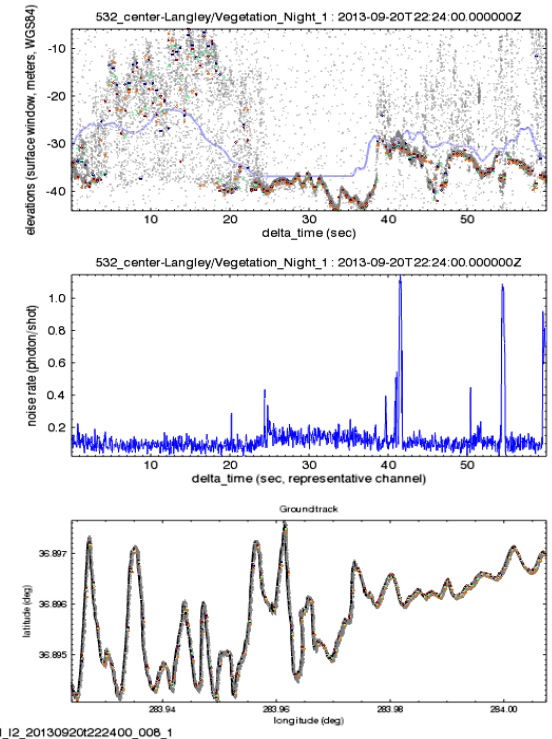


**Figure 2: Raw MABEL data.** MABEL data collected during the campaign. This plot represents the elevation recorded through 60 seconds of time, or approximately 7.5 km distance, as covered by the Proteus. In the upper panel, trees are clearly distinguishable on either side of what is probably a large body of water (blue line is the estimated surface from a digital elevation map). These data are not yet corrected for aircraft pitch/yaw/roll. The red line indicates where a surface was found by MABEL's automated surface finding routines. Note, the ground is hidden under the denser canopy. (Data reduction and plots provided by D. Hancock, NASA/WFF.)



Name: William B. Cook, NASA/GSFC, Code 612  
E-mail: william.b.cook@nasa.gov  
Phone: 301-614-7123

### **Additional Credits:**

Kelly Brunt (615/GSFC & Morgan State U.) provided detailed flight planning and weather prediction support in the field. The MABEL team at NASA LaRC also included Eugenia DeMarco, Dan Reed (both from SigmaSpace), and Mark Shappirio (NASA/GSFC). Excellent facilities and much-appreciated ground support were provided by NASA LaRC. Proteus, the pilots, and crew from Scaled Composites were a pleasure to work with at all stages of the project, and they contributed significantly towards the technical success of the campaign. We also acknowledge the full cooperation we received from the USAF in providing ready access to the runway and ground support.

### **Technical Description of Figures:**

**Figure 1:** The targets and flights paths used by Proteus/MABEL are shown in red (from web site data indicating where the ground was detected). Flight paths were repeated for each flight, but most targets were traversed in reverse directions on alternate flights (helpful for calibration). Two flights occurred at dusk/night, and two flights during the middle of the day. Night vs. day data will be used to evaluate the effects of solar background on the retrievals. Cloud conditions were variable and this was desired since one goal of the eventual analyses is to determine effects of clouds on the retrieved canopy parameters.

**Figure 2:** The MABEL data contains both laser photons and solar reflected photons that are at wavelengths allowing them to pass through the spectrally narrow etalon filter. The upper panel shows the raw (uncorrected for aircraft/instrument motion) elevation estimates for each photon received by MABEL. The middle panel is an estimate of the background/noise rate. The lower panel shows the latitude and longitude of the nadir point beneath the Proteus. Proteus flew at an altitude of 46,000 feet, so turbulence and the positioning of MABEL in the pod underneath the fuselage (rather than within it as on ER-2) led to a bumpy ride and more pointing variability in comparison with previous flights aboard ER-2 at 63,000 feet. Once corrected using our IMU and GPS information, we expect to see very little difference in final elevation precision. MABEL is configured differently in the Proteus pod than in previous flights (reversed orientation, some different IFOV selections, etc.) so we need to re-calibrate MABEL's pointing parameters, and this is still in progress. We expect to have improved MABEL's pointing knowledge through discovery and use of additional internal error information we now collect and store from the IMU – new algorithms are being developed to incorporate this information into our correction procedure. We expect to have this completed soon and applied to create a new release of better-corrected campaign data sometime in December 2013.

**Figure 3:** MABEL is in the pod hanging underneath the Proteus. Access ports built into the pod allow us to retrieve flight data and perform between-flight maintenance without opening it. The pod can hold MABEL and the NASA/GSFC Cloud Physics Lidar (CPL). Both versions of CPL had other commitments during our mission timeframe, and so CPL was not flown with MABEL this time. Scaled Composites built the pod to our specifications, which were generically developed to support any nose-cone and any wing pod instrument currently flown aboard ER-2. The construction, testing, and most of the design work for the pod was funded by NASA Airborne Sciences.

**Scientific significance:** The NASA LaRC campaign was the first successful concentrated MABEL deployment designed to produce vegetation canopy data for algorithm development for ICESat-2. Prior successful MABEL missions were primarily for engineering verification and demonstration of the technique, and the April 2012 Iceland-based campaign over snow/ice targets in Greenland. Many recent repairs and upgrades to MABEL systems (primarily computer and electronic) have paid off and MABEL is now fully functional and more robust than ever.

**Relevance for future science and NASA missions:** The data collected by MABEL will enable the development of the science algorithms needed for the ICESat-2 mission. The signal acquired by the photon counting technique to be employed by ICESat-2/ATLAS differs significantly from the signals acquired during ICESat by GLAS, and so new analysis techniques and algorithms are required. MABEL closely simulates the data expected from the ICESat-2/ATLAS instrument in both spatial and temporal formats. During the next few years we will improve our understanding of MABEL and use MABEL for fundamental science associated with ice, snow and perhaps vegetation in support of the ICESat-2 and other missions.



# How do clouds overlap? New insights from active satellite observations

Tianle Yuan and Lazaros Oreopoulos, Code 613, NASA-GSFC and UMBC-JCET



Thin high clouds and low boundary layer clouds are two important cloud types for the Earth's radiation budget. Thin high clouds trap outgoing thermal infrared (IR) radiation and thus exert a net warming effect since they have only a minor influence on solar radiation. Low boundary layer clouds, on the other hand, strongly impact reflected solar radiation while only weakly changing the thermal IR radiation emitted to space, and therefore cool the planet. A variety of evidence suggests that these vertically well-separated cloud types often coexist in the same geographic area. In this type of high-over-low-cloud overlap, the net radiative impact of the two cloud types as seen from space largely cancels out. Furthermore, the presence of high clouds can significantly modify the strength of IR cooling at the top of low clouds which strongly affects their development.

In a recent paper (Yuan and Oreopoulos 2013) we studied the global features of high-over-low cloud overlap using observations from the CloudSat and CALIPSO satellites carrying radar and lidar instruments, respectively. Near-global maps of cloud overlap rate can be produced using our methods (Fig. 1). We found three major regimes of overlap, in areas of tropical convection, Hadley cell large-scale descent, and midlatitude storm prevalence. These regimes exhibit seasonal variations (Fig. 2) due to circulation shifts. In our paper we also document other intriguing results not shown here. We found that overlap rate scales linearly with the rate of large-scale vertical motion (obtained from MERRA), so that weaker ascent or stronger descent means less overlap. We also found that the vertical separation of the two cloud layers follows the zonal variations of tropopause height. All these results should be reproducible by Global Climate Models claiming good cloud simulations.

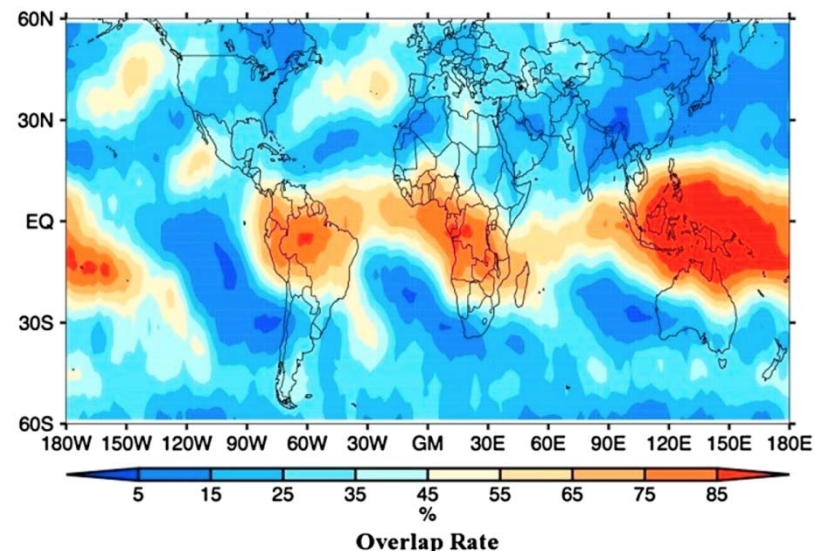


**Figure 1:** Map of overlap rate for January 2009 from combined CloudSat-CALIPSO data.

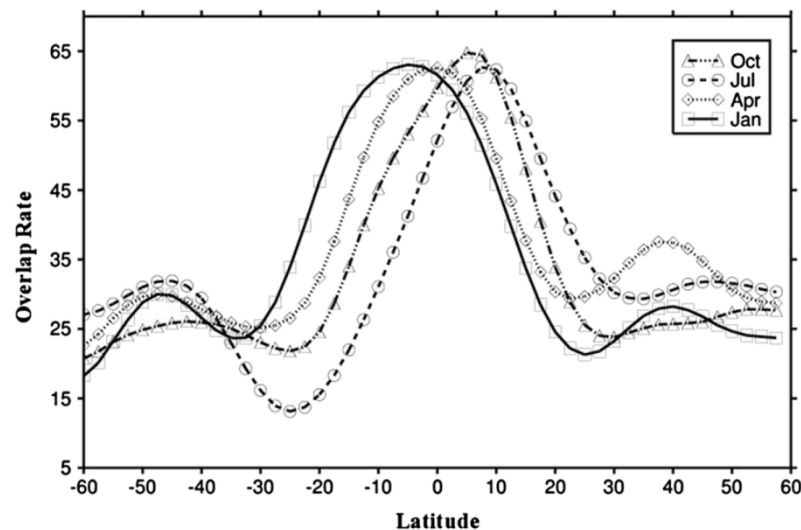


**Figure 2:** Latitudinally-averaged mean overlap rate for four months representing different seasons using the same data set as in Fig. 1.



Name: Tianle Yuan, NASA/GSFC, Code 613 and UMBC-JCET  
E-mail: Tianle.Yuan@nasa.gov  
Phone: 301-614-6195



### References:

- Yuan, T., and L. Oreopoulos (2013), On the global character of overlap between low and high clouds, *Geophysical Research Letters*, 40, 5320–5326, doi:10.1002/grl.50871.
- Oreopoulos, L., D. Lee, Y. C. Sud, and M. J. Suarez (2012), Radiative impacts of cloud heterogeneity and overlap in an atmospheric General Circulation Model, *Atmospheric Chemistry and Physics*, 12, 9097-9111, doi:10.5194/acp-12-9097-2012.

**Data Sources:** 2B-GEOPROF-LIDAR product, a merged product from CloudSat and CALIPSO, CALIPSO 1 km cloud layer product, and MERRA re-analysis data.

### Technical Description of Figures:

**Figure 1:** Geographical distribution of the cloud overlap rate, defined as the ratio of the number of profiles with overlap to the number of low-cloud profiles, based on the merged CloudSat/CALIPSO 2B-GEOPROF-LIDAR product. Maxima can be seen in the tropical convective areas, in particular the Pacific Warm Pool and surrounding “maritime continent” where overlap rates of 80% are common. Minima are generally found over some land areas and over oceanic areas dominated by marine stratocumulus, where values can drop as low as 5%. These are regions of persistent strong subsidence, generally unfavorable for upper-level cloud formation, but high clouds can still form under favorable conditions, due to topography-driven gravity wave activity, advection from neighboring tropical convection centers such as the Amazon and Congo basins, or ascent in neighboring midlatitude fronts, yielding overlap rates up to 25%. In the midlatitude storm track regions themselves, intermediate values between 35% to 65% are encountered, in accordance with recent findings of thin cirrus presence in cyclonic systems. The global overlap rate is 30% in January 2009, slightly higher over land (32.6%) than ocean (28.5%).

**Figure 2:** The three clearly discernible regimes discussed above (subsidence, convective and midlatitude storm areas) collectively result in a zonal mean pattern which exhibits one major peak in the tropics, two minor peaks in the midlatitudes, and two local minima in the subtropics. This overall pattern shifts seasonally as shown by the four curves, one for each month representative of a season. The seasonal shift of tropical convection manifests itself as a zonal shift in overlap rate maxima with the peak values staying about the same. In contrast, the magnitude of subtropical minima undergoes much more substantial seasonal changes, something that warrants further investigation. A strong, but curious, springtime local maximum in the northern midlatitudes may be the result of high-level dust being misidentified as high ice clouds, or may be exposing actual dust influence on ice nucleation.

**Scientific significance:** One of the least well-known aspects of global cloudiness, at least until recently, is cloud vertical distribution. Detecting multi-layer cloud systems from space is extremely difficult with passive radiometers (but still possible under certain conditions) measuring reflected solar radiation or emitted thermal infrared radiation. Despite their own limitations, active space sensors, namely lidars and cloud/precipitation radars are much more capable in discerning complex vertical cloud structures. This paper is a significant contribution towards building an observed climatology of how clouds overlap in the vertical, information to be used by Global Climate Models when assessing how well they simulate this particular cloud property. A less studied, but nevertheless important topic is the radiative impact of cloud overlap at the thermal infrared part of the spectrum where the radiative interactions between multiple cloud layers is expected to alter their lifecycle (especially for low clouds) compared to the situation where clouds tops are exposed to space.

**Relevance to future science and NASA missions:** Results of the kind shown here demonstrate the utility and power of putting lidars and radars in space, especially when they can observe the same locations on Earth at the same time. The forthcoming EarthCare mission, a joint venture between the European and Japanese space agencies is capable of such simultaneous measurements. However, from the US side, only if the Decadal Survey’s ACE materializes will such capabilities be recovered after the inevitable demise of A-Train’s CloudSat and CALIPSO satellites.



# New Algorithm Vastly Improves Measurements of SO<sub>2</sub> Pollution from Space

Can Li, Joanna Joiner, Nickolay A. Krotkov, Pawan K. Bhartia, Code 614, NASA GSFC

Sulfur dioxide (SO<sub>2</sub>), predominantly emitted from man-made activities, can significantly impact air quality and climate. Advanced sensors including the Ozone Monitoring Instrument (OMI) flying on NASA's Aura spacecraft have been employed to measure SO<sub>2</sub> pollution. However existing algorithms often have substantial noise and biases (*cf.* Figs. 1b and 2b) owing to relatively weak signals and various interferences such as ozone absorption and stray light.

We have developed a fundamentally different approach for retrieving SO<sub>2</sub> from satellites. It has the following advantages:

- ✓ It reduces retrieval noise by a factor of two compared with the operational OMI algorithm. Biases also become much smaller (*cf.* Figs. 1a and 2a). This vastly enhances sensitivity to weak anthropogenic sources;
- ✓ It utilizes hundreds of wavelengths available from OMI, but only requires 4-5 minutes to process an entire orbit on a single CPU, more than an order of magnitude faster than comparable methods that rely on on-line radiative transfer calculations;
- ✓ It can be easily applied to new instruments such as the Suomi National Polar Partnership (NPP) Ozone Mapping and Profiler Suite (OMPS), because it eliminates the need to develop empirical data correction schemes for each individual instrument.

This new algorithm will allow high quality, consistent SO<sub>2</sub> data to be produced from different satellites, ensuring continuity in long-term SO<sub>2</sub> records for climate and air quality research.

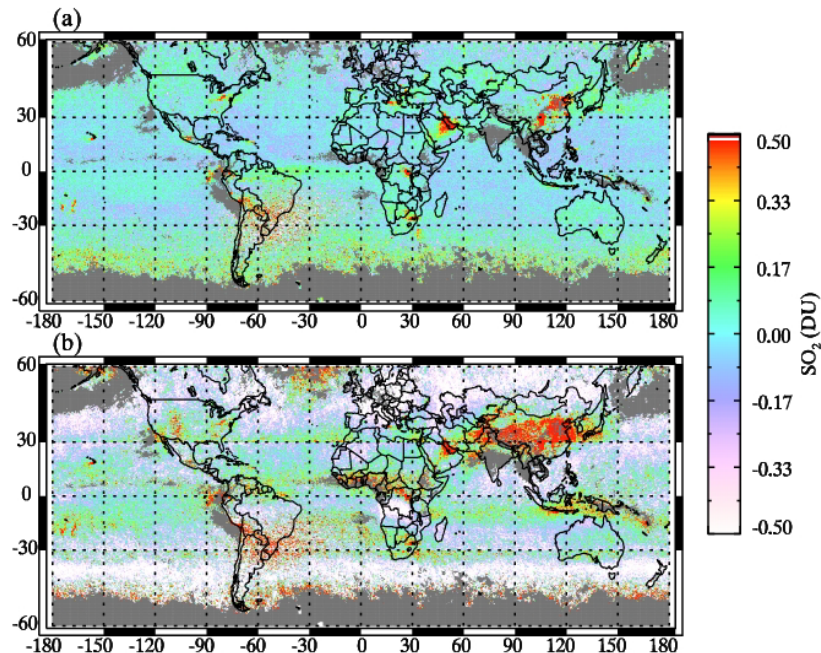


**Figure 1:** Monthly mean SO<sub>2</sub> maps for August 2006 generated from OMI data using (a) the new algorithm and (b) the operational algorithm. Colors represent the amount of SO<sub>2</sub> in the atmospheric column above the surface in Dobson Unit (DU). 1 DU means  $2.69 \times 10^{16}$  SO<sub>2</sub> molecules above a surface of 1 cm<sup>2</sup>. Negative values represent retrieval biases that are greatly reduced in the new algorithm.

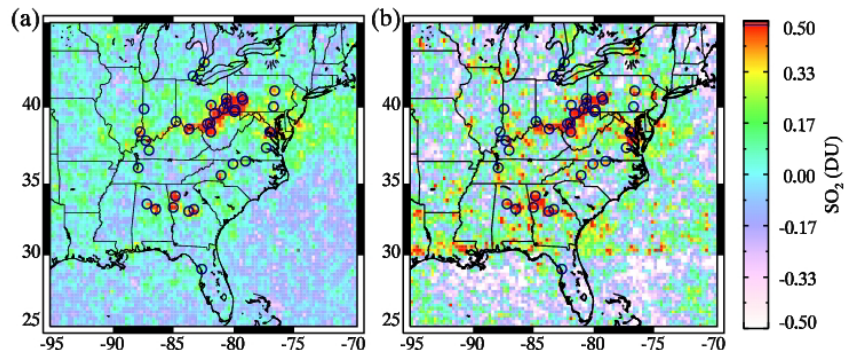


**Figure 2:** Same as in Figure 1 but over the eastern U.S. using (a) the new algorithm and (b) the operational algorithm. Circles represent large SO<sub>2</sub> sources (e.g., coal-fired power plants) that emit more than 70,000 tons of SO<sub>2</sub> annually.



Name: Can Li, NASA/GSFC, Code 614 and UMD/ESSIC

E-mail: can.li@nasa.gov

Phone: 301-614-5616

### References:

Li, C., J. Joiner, N. A. Krotkov, P. K. Bhartia (2013), A fast and sensitive new satellite SO<sub>2</sub> retrieval algorithm based on principal component analysis: Application to the Ozone Monitoring Instrument, *Geophysical Research Letters*, doi:10.1002/2013GL058134, in press.

(<http://onlinelibrary.wiley.com/doi/10.1002/2013GL058134/abstract>)

**Data Sources:** NASA/KNMI OMI L1B radiance data and L2 PBL SO<sub>2</sub> and total O<sub>3</sub> data (<http://disc.gsfc.nasa.gov/>).

### Technical Description of Figures:

**Figure 1: (a)** Monthly mean SO<sub>2</sub> for August 2006 retrieved using our new principal component analysis (PCA) algorithm. Data were gridded to 0.25°x0.25°. Pixels outside the center 50 OMI CCD detector rows, or with radiative cloud fraction > 0.3 or slant column O<sub>3</sub> > 1500 DU are excluded. Gray-shaded grid cells have less than 5 measurements during the month. **(b)** Same as in (a) but for the operational OMI L2 PBL SO<sub>2</sub> data. Both retrievals assumed the same ozone, SO<sub>2</sub>, and temperature profiles, as well as the same surface albedo, surface pressure, and solar zenith and viewing zenith angles. This allows a fair intercomparison between the new and operational algorithms. Biases in the operational product, for example, the unrealistic large negative values in the northern high latitudes and positive values over the Tibet and the Rocky Mountains in (b) are largely eliminated in the new retrievals in (a). Over the clean remote oceanic regions (e.g., the central Pacific) one would expect SO<sub>2</sub> loading to be close to zero (represented by blue color).

**Figure 2: (a)** Monthly mean SO<sub>2</sub> for August 2006 over the eastern U.S. retrieved using our new PCA algorithm. Solid circles mark the locations of some major SO<sub>2</sub> point sources (> 70 kt/yr). **(b)** Same as in (a) but for the operational OMI L2 PBL SO<sub>2</sub> product. Smaller noise and biases in the new retrievals allow large point SO<sub>2</sub> sources to be more clearly distinguished. Smaller stationary SO<sub>2</sub> sources may also be detected by the new PCA algorithm, but likely will require data averaging over a longer period of time.

**Scientific significance:** The reduced noise and low biases in SO<sub>2</sub> retrievals achieved in the new algorithm will allow SO<sub>2</sub> pollution to be monitored at much greater temporal resolution and will enable the detection of smaller emission sources. This can be particularly important in light of the recent reduction in SO<sub>2</sub> emissions in many regions around the world, including the U.S. The new algorithm can also minimize the differences between SO<sub>2</sub> data records from different satellite sensors, making it possible to produce consistent long-term datasets necessary for climate research. Finally, the new algorithm offers a framework to efficiently utilize the rich spectral information from the state-of-the-art space-borne spectrometers, with minimal required additional computation. Unlike the existing methods that attempt to model different interferences such as ozone absorption and stray light, we directly extract characteristic features from satellite radiance data to account for them, using a principal component analysis technique. This reduces modeling errors and makes the algorithm much faster. It may also be employed to retrieve several other species such as formaldehyde (HCHO).

**Relevance for future science and NASA missions:** The new algorithm has been proposed to reprocess data from the Aura OMI mission. It can be applied to NPP and future JPSS OMPS instruments to ensure SO<sub>2</sub> data continuity from the EOS era. It can also help extend satellite SO<sub>2</sub> data records if applied to other current and future NASA and European missions such as TEMPO, GEO-CAPE, TROPOMI and GOME-2. TEMPO is the first selected NASA EVI instrument and will be launched on a geostationary platform near the end of the decade.